AIP | The Journal of Chemical Physics

The impact of electron correlations on the energetics and stability of silicon nanoclusters

N. L. Matsko, E. V. Tikhonov, V. S. Baturin, S. V. Lepeshkin, and Artem R. Oganov

Citation: The Journal of Chemical Physics **145**, 074313 (2016); doi: 10.1063/1.4960675
View online: http://dx.doi.org/10.1063/1.4960675
View Table of Contents: http://scitation.aip.org/content/aip/journal/jcp/145/7?ver=pdfcov
Published by the AIP Publishing

Articles you may be interested in

Half-metallicity and spin-contamination of the electronic ground state of graphene nanoribbons and related systems: An impossible compromise?
J. Chem. Phys. **135**, 104704 (2011); 10.1063/1.3626554

Influence of electronic correlations on the ground-state properties of cerium dioxide
J. Chem. Phys. **124**, 234711 (2006); 10.1063/1.2206187

Evolution of the electronic structure of Be clusters
J. Chem. Phys. **123**, 074329 (2005); 10.1063/1.2001655

Equilibrium geometries of low-lying isomers of some Li clusters, within Hartree–Fock theory plus bond order or MP2 correlation corrections
J. Chem. Phys. **120**, 11615 (2004); 10.1063/1.1729954

Electronic structure and chemical bonding of B 5 − and B 5 by photoelectron spectroscopy and ab initio calculations
J. Chem. Phys. **117**, 7917 (2002); 10.1063/1.1511184

Reuse of AIP Publishing content is subject to the terms: https://publishing.aip.org/authors/rights-and-permissions. Downloaded to IP: 91.103.211.186 On: Fri, 26 Aug 2016 16:29:05

The impact of electron correlations on the energetics and stability of silicon nanoclusters

N. L. Matsko,[1,2] E. V. Tikhonov,[2,3] V. S. Baturin,[1,2] S. V. Lepeshkin,[1,2] and Artem R. Oganov[2,4,5,6]
[1]*P.N. Lebedev Physical Institute, Russian Academy of Sciences, Leninskii Prosp. 53, 119991 Moscow, Russia*
[2]*Moscow Institute of Physics and Technology, Dolgoprudny, Moscow Region 141700, Russia*
[3]*Lomonosov Moscow State University, Leninskie Gory, Moscow 119991, Russia*
[4]*Skolkovo Institute of Science and Technology, Building 3, Moscow 143026, Russia*
[5]*Northwestern Polytechnical University–Xi'an, Shaanxi 710072, People's Republic of China*
[6]*Department of Geosciences and Center for Materials by Design, Institute for Advanced Computational Science, State University of New York, Stony Brook, NY 11794-2100, USA*

(Received 13 April 2016; accepted 26 July 2016; published online 19 August 2016)

The first-principles prediction of stable nanocluster structure is often hampered by the existence of many isomer configurations with energies close to the ground state. This fact attaches additional importance to many-electron effects beyond density functional theory (DFT), because their contributions can change a subtle energy order of competitive structures. To analyze this problem, we consider, as an example, the energetics of silicon nanoclusters passivated by hydrogen $Si_{10}H_{2n}$ ($0 \le n \le 11$), where passivation changes the structure from compact to loosely packed and branched. Our calculations performed with DFT, hybrid functionals, and Hartree-Fock methods, as well as by the GW approximation, confirm a considerable sensitivity of isomer energy ordering to many-electron effects. *Published by AIP Publishing.* [http://dx.doi.org/10.1063/1.4960675]

I. INTRODUCTION

Application of semiconductor nanoparticles is of considerable promise for optoelectronics, nanoelectronics, solar cells, biosensors, etc.[1–5] One of the challenging problems is the atomic structure of nanoclusters and small nanoparticles, which generally differs great from the structure of bulk samples and varies widely with cluster size and composition. Nano-object structure strongly affects its properties. The minimization of the total energy triggers atom rearrangement making the structure unique for each cluster. The experimental determination of nanocluster structure is still problematic, so reliable first-principles structure prediction is among the hottest problems of nanocluster physics.

First-principles calculation based on density functional theory (DFT) received general recognition as a common research method for a wide class of materials, including nanoclusters, nanomaterials, and prediction of the stable structure of nano-objects.[6–8] From a mathematical point of view, the determination of a cluster structure is reduced to a search for the atomic configuration realizing the global energy minimum. This search is especially difficult when a system has many local minima lying slightly above the global one. In this case, any inaccuracy or a small systematic error can distort a subtle energy order of atomic configurations. Of course, there is a reasonable limit of accuracy. When isomer configurations have energy difference close to $k_B T_{eff}$ (about 0.03 eV at room temperature), structures get comparable chances to exist and the notion of the ground state is blurred.

In first-principles calculations, an evident source of systematic errors is the exchange-correlation (xc) contribution. This contribution is subject to approximation: from the standard local-density approximation (LDA) and generalized gradient approximation (GGA)[9,10] to the beyond-DFT methods. Thus, the employed approximation causes characteristic shifts in the energies of the atomic structures of the nanoclusters under study. The important question is whether these shifts are nearly the same for each configuration. If this is not the case, proper description of many-electron effects becomes essential.

To elucidate this question, we perform total energy calculations for silicon nanoclusters with the formula $Si_{10}H_{2n}$ ($0 \le n \le 11$), passivated by hydrogen, using different xc approximations. According to our earlier first-principles studies,[11,12] the equilibrium structure of these clusters varies widely from very compact (Si_{10}) to loosely packed and branched ($Si_{10}H_{22}$) (Figure 1). The characteristic differences −7 of energy for atomic configurations also vary greatly with hydrogen passivation. As an example, in bare Si_{10} clusters, the first isomer energy lies at 0.6 eV above the ground state, while in $Si_{10}H_{22}$ clusters, this quantity falls to 0.04 eV. Such diversity of structures and energetics renders the $Si_{10}H_{2n}$ family very suitable for studying the effect of xc refinements on cluster structure prediction. The calculations were performed for both the ground-state and low-energy isomer configurations using the GGA, hybrid functionals, Hartree-Fock (HF), and GW methods. 31 cluster configurations corresponding to seven cluster compositions were calculated, which gave valuable information about the impact of many-electron effects on cluster structure prediction.

Besides, it should be mentioned that hybrid functionals are often considered as a very accurate approach for the description of nanoclusters, especially B3LYP.[16–20] On the other hand, these works give no reasons for the validity of

Reuse of AIP Publishing content is subject to the terms: https://publishing.aip.org/authors/rights-and-permissions. Downloaded to IP: 91.103.211.186 On: Fri, 26 Aug 2016 16:29:05

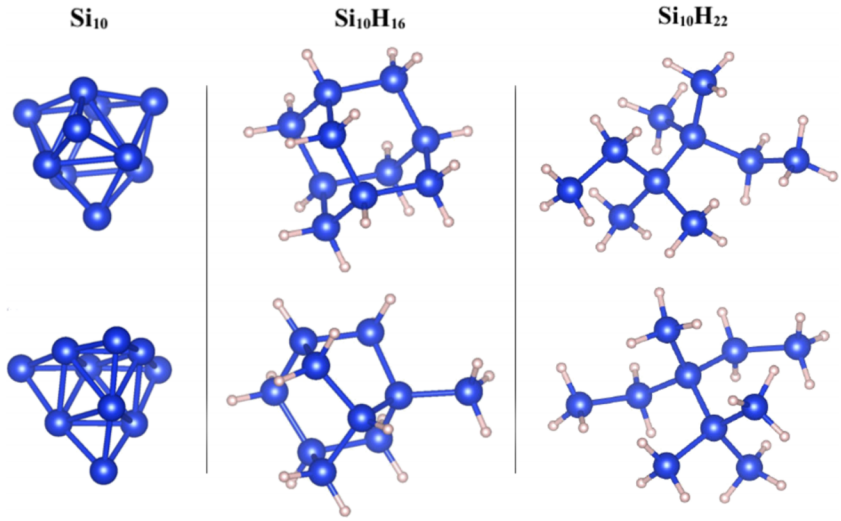

FIG. 1. Ground state structures (upper line) and closest isomers (bottom line) of Si_{10}, $Si_{10}H_{16}$, and $Si_{10}H_{22}$ nanoclusters. Large dark spheres—silicon atoms, small pale spheres—hydrogen atoms.

such approaches. In works,[13–15] quantum Monte Carlo (QMC) method was applied to calculate total energy of some silicon nanoclusters, it was shown that proper description of the electron correlation effects can significantly affect nanocluster energetics.

The paper proceeds as follows. Section II gives the basic formulas and discusses the physical meaning of the approximations relating to many-electron effects. Section III considers the details of computation, while Section IV checks the accuracy of our GW calculations. Section V presents polarizabilities and total energies of $Si_{10}H_{2n}$ nanoclusters. The discussion of these results reveals the sensitivity of structure prediction to refinements in the description of electron exchange and correlations.

II. THEORY

The exchange-correlation energy in DFT GGA is

$$E_{\rm xc}^{\rm GGA}[\rho] = \int d\mathbf{r}\rho(\mathbf{r})\epsilon_{\rm xc}(\rho(\mathbf{r}),\nabla\rho(\mathbf{r})), \quad (1)$$

where density of exchange-correlation energy $\epsilon_{\rm xc}(\mathbf{r})$ is a function of electron density $\rho(\mathbf{r})$ and its gradient at point $\mathbf{r}$. This approximation is static and local and does not include interactions between the electron density perturbations in various parts of the system. The GGA works well for metals, where screened Coulomb interaction is short-range, which makes xc interaction rather local. In semiconductors and dielectrics, the screened Coulomb interaction decreases very slowly with distance, thus the use of local and semi-local approximations (the DFT LDA and GGA) is not well-justified.

The Hartree-Fock approximation accounts for electron exchange explicitly. It is not local but also static and in terms of the density matrix $\rho(\mathbf{r},\mathbf{r}')$ is

$$E_{\rm x}^{\rm HF} = -\frac{1}{2}\int {\rm d}\mathbf{r}{\rm d}\mathbf{r}'\frac{\rho(\mathbf{r},\mathbf{r}')\rho(\mathbf{r}',\mathbf{r})e^2}{|\mathbf{r}-\mathbf{r}'|}. \quad (2)$$

The HF approximation neglects the contribution of electron correlations. This inadequacy is partially compensated by hybrid functionals. They take into account HF exchange and consider contribution from electron correlations approximately (usually in the form of the LDA or GGA). The simplest hybrid functional can be written[21] as

$$E_{\rm xc}^{\rm hyb} = \alpha_{\rm mix}E_{\rm x}^{\rm HF} + (1-\alpha_{\rm mix})E_{\rm x}^{\rm GGA}[\rho] + E_{\rm c}^{\rm GGA}[\rho]. \quad (3)$$

The hybrid functional (3) depends on one free parameter $\alpha_{\rm mix}$, which is usually taken close to 0.25 (the PBE0[22,23] functional). In most cases, the accuracy of (3) is higher than that of the LDA and GGA. More sophisticated hybrid functionals B3PW91, B3LYP, HSE, and etc.,[24–27] have three or more parameters, giving additional flexibility for the description of exchange and correlation.

The GW approximation (GWA) takes into account both the exact exchange and electronic correlations, including static and dynamic ones and disregarding vertex corrections. The energies of electronic quasiparticles (QP) ϵ_i are the eigenvalues of the Dyson equation,

$$\left[\frac{p^2}{2m} + V_{\rm ext}(\mathbf{r}) + V_{\rm H}(\mathbf{r})\right]\phi_i(\mathbf{r}) + \int {\rm d}\mathbf{r}'\Sigma(\mathbf{r},\mathbf{r}',\epsilon_i)\phi_i(\mathbf{r}') = \epsilon_i\phi_i(\mathbf{r}). \quad (4)$$

In the GWA, the self-energy operator (SEO) Σ is given by the expression

$$\Sigma(\mathbf{r},\mathbf{r}',\omega) = \frac{i}{2\pi}\int {\rm d}\omega' G(\mathbf{r},\mathbf{r}',\omega+\omega')W(\mathbf{r},\mathbf{r}',\omega'). \quad (5)$$

Here $W(\mathbf{r},\mathbf{r}',\omega)$ and $G(\mathbf{r},\mathbf{r}',\omega)$ are, respectively, the dynamically screened Coulomb interaction and the one-electron Green's function. In many cases, it is convenient to use the Lehmann spectral representation of $G(\mathbf{r},\mathbf{r}',\omega)$,

$$G(\mathbf{r},\mathbf{r}',\omega) = \int_{-\infty}^{\infty}{\rm d}\omega'\frac{A(\mathbf{r},\mathbf{r}',\omega)}{\omega-\omega'-i\delta\cdot sgn(\mu-\omega')}, \quad (6)$$

where μ is the chemical potential and $A(\mathbf{r},\mathbf{r}',\omega)$ is the electron spectral function. Using spectral representation, we can write the Galitskii-Migdal (GM) formula[28,29] for the total energy of the electron system,

$$E^{GM} = \frac{1}{2}\int_{-\infty}^{\mu}{\rm Tr}\{[\omega+h]A(\omega)\}{\rm d}\omega, \quad (7)$$

Reuse of AIP Publishing content is subject to the terms: https://publishing.aip.org/authors/rights-and-permissions. Downloaded to IP: 91.103.211.186 On: Fri, 26 Aug 2016 16:29:05

where h is the one-particle part of the Hamiltonian: the sum of the kinetic energy operator and the external potential.

For the use of the GM formula (7) we need the spectral function $A(\omega)$. This function has peaks at QP energies and important features in the spectrum (satellites), which arise from dynamical interaction of electrons due to plasmon exchange. The valence-band plasmon satellites manifest themselves as peaks positioned at multiples of the plasmon energy below each quasiparticle level ϵ_i.[30–32] For the satellite description, a model spectral function can be employed, where an electron at the level i interacts with a plasmon having the plasma energy ω_p, the satellite series is assumed infinite.[30] Then the GM GWA total energy correction to DFT can be given as

$$E^{\mathrm{GM}} - E^{\mathrm{DFT}} = \frac{1}{2}\left[\sum_i n_i(\epsilon_i^{QP} - \epsilon_i^{DFT}) + N\omega_p|\ln \overline{Z}| + \int \mathrm{d}\mathbf{r}\rho(\mathbf{r})V_{\mathrm{xc}}\right] - E_{\mathrm{xc}}[\rho], \quad (8)$$

where n_i is the occupation number, ϵ_i^{QP} is the quasiparticle energy calculated by the GWA, N is the total number of electrons in a nanocluster, Z_i is the renormalization factor, and $\ln \overline{Z} = \Sigma_i\, n_i \cdot \ln Z_i/N$, where $0 < Z_i \leq 1$. Because electron density, averaged over a cluster, varies only slightly from one isomer configuration to another, we expect that the second term of (8) (the satellite contribution) is nearly invariant under atom rearrangements and affects the energy differences between isomers very weakly. This point is explored deeper in Sections III and IV.

It is also of interest to examine correlation between polarizabilities and energetics of nanoclusters. Dielectric properties of a system reflect its interaction with external and internal electric field, electron screening, and affect system energy as well. According to the adiabatic connection fluctuation-dissipation theorem (ACFDT),[33–35] the correlation energy can be expressed as

$$E_C = -\int_0^1 \mathrm{d}\lambda \int_0^\infty \frac{\mathrm{d}\omega}{2\pi} Tr\{\mathrm{v}[\chi^\lambda(i\omega) - \chi^0(i\omega)]\}, \quad (9)$$

where λ is a dimensionless coupling constant ($\lambda = 0$ for the case of noninteracting electron system and $\lambda = 1$ for the real physical system), χ is the electron response function, v denotes Coulomb interaction. It can be seen that correlation energy of a system increases when χ^λ, being negative, increases in absolute value. In the GWA SEO (5), screened Coulomb W can be rewritten as $\epsilon^{-1}(q,\omega) \times \mathrm{v}(q)$, where $\epsilon^{-1}(q,\omega)$ is an inverse dielectric function, thus in GWA dielectric properties of the electron system also affect computation results. According to these simple considerations, it seems reasonable to expect that isomers for a given molecular formula with greater $|\chi^\lambda|$ have, in general, higher total energy. Hence they are energetically less favorable. Although ϵ and χ functions depend on frequency, it can be considered that the static polarizability roughly represents the dielectric response of the system. Calculation of the static polarizability is implemented in many DFT packages and is much less time consuming than calculations on the GWA level. The consideration of the relationship between total energies of Si_7 and $Si_{10}H_{2n}$ isomers and their static polarizabilities will be examined in Sections IV and V.

III. COMPUTATIONAL METHODOLOGY

Our density functional calculations were performed with the DFT GGA xc functional using the Quantum Espresso (QE)[36] and VASP[37–40] codes. The QE calculations were made using Perdew-Burke-Ernzerhof (PBE) pseudopotential and a plane wave basis set having the cutoff energy of 50 Ry, while VASP's ones were done with the projector-augmented wave (PAW) basis set, cutoff energy of 500 eV, and appropriate pseudopotential.[41,42] Computations were performed for the supercell geometry with the vacuum region of 13 Å between nano-object replicas (Section IV discusses this choice). A nontrivial determination of cluster geometry was made with the evolutionary algorithm realized in the USPEX code,[43,44] as has been described in our previous publications.[11,12] The atomic structure of considered molecules and nanoclusters was relaxed using PBE GGA functional until atomic forces became less than 10^{-4} Ry/Å. Both the Hartree-Fock and hybrid functional (PBE0 and B3LYP) calculations were performed using the QE code with the parameters described above.

Methods based on the GW approximation could be ranked by the level of self-consistency. In this way, G_0W_0 is the simplest method. G_0 is usually picked as the DFT, Hartree-Fock, or hybrid functional Green function, $W_0(\mathbf{r},\mathbf{r}',t) = W[G_0]$ and $\Sigma_0(\mathbf{r},\mathbf{r}',t) = iG_0(\mathbf{r},\mathbf{r}',t)W_0(\mathbf{r},\mathbf{r}',t)$. Quasiparticle energies are obtained from the expression $E_{\mathrm{QP}} = E_{\mathrm{QP}}^{\mathrm{DFT}} - \langle\psi|V_{\mathrm{xc}}|\psi\rangle + \Sigma(E_{\mathrm{QP}}^{\mathrm{DFT}})$. The QP spectrum found at this step is much more accurate than Kohn-Sham spectrum. In particular, the HOMO-LUMO gap of semiconductor nano-objects calculated in the G_0W_0 approximation is rather close to the experimental gap, while the DFT gap is 2-3 times narrower.[45,48–50] Elementary improvement can be obtained by getting QP energies as $E_{\mathrm{QP}} = E_{\mathrm{QP}}^{\mathrm{DFT}} - \langle\psi|V_{\mathrm{xc}}|\psi\rangle + \Sigma(E_{\mathrm{QP}})$ and making iterations of the substitutions E_{QP} to Σ for the next step until convergence is achieved (self-consistency in the eigenvalues or ev-scGW). Further improvement can be obtained as an iterative solution of Dyson equation with the SEO $\Sigma(\mathbf{r},\mathbf{r}',t) = iG(\mathbf{r},\mathbf{r}',t)W_0(\mathbf{r},\mathbf{r}',t)$, where only the Green's function is iterated to the self-consistency at fixed W_0 (the $scGW_0$). Fully self-consistent scGW is obtained when Dyson equation is iterated both on G and W. In principle, full self-consistency eliminates errors of the start point and leads to the fulfillment of conservation laws for the total energy, momentum, and number of particles.[51,52] In Refs. 53–55, it was noticed that fully self-consistent GW improves the G_0W_0 total energy and ionization potentials, significantly improving the DFT and hybrid functional results. However both approximations (G_0W_0 and GW_0) greatly decrease the amount of computation and yet provide accurate quasiparticle spectra. It has been observed that sometimes the simpler G_0W_0 and GW_0 methods provide even better spectra than the fully self-consistent GW calculation.[56–58] This fact is explained by partial cancelation between vertex correction diagrams and the self-consistency effects.[59] According to formula (7), exact quasiparticle spectra give accurate total energies.

Reuse of AIP Publishing content is subject to the terms: https://publishing.aip.org/authors/rights-and-permissions. Downloaded to IP: 91.103.211.186 On: Fri, 26 Aug 2016 16:29:05

For the GWA calculations, two packages were used: BerkeleyGW[45,60,61] and VASP. In both cases for all calculations, the starting point was DFT GGA eigenfunctions and eigenvalues calculated with VASP PAW for the VASP $scGW_0$ and with QE PBE for the case of BerkeleyGW G_0W_0 and ev-scGW calculations. The VASP GW algorithm performs a direct inversion of the dielectric matrix on a frequency grid. The BerkeleyGW package can employ both the direct inversion of the dielectric matrix and the Generalized Plasmon Pole (GPP) model[45] (GPP accelerates calculations and reduces computer memory demands). The nonuniform frequency grid for the direct inversion of the dielectric matrix in the VASP computations consisted of 50 points and of 200 points for the BerkeleyGW, the dielectric matrix was cut off at 300 eV. In the BerkeleyGW GPP dielectric matrix was cut off at 6 Ry in the momentum space. When computing the self-energy operator of the GWA, we performed summation over all occupied and 600 unoccupied electron states.

GW_0 and ev-scGW require notable extra resources, therefore these methods were applied only for small nano-objects—ethyl and dimethyl ether molecules, Si_3 and Si_6 nanoclusters. BerkeleyGW dielectric matrix direct inversion computations were applied only for the study of the plasmon satellites in the ethyl and dimethyl ether molecules and the Si_7 clusters. The GW calculations of $Si_{10}H_{2n}$ clusters were performed with the BerkeleyGW G_0W_0 GPP approximation.

In this paper, when calculating relative energies of nanocluster isomers with the GM formula, we will neglect plasmonic modifications in the spectral function. $A(\omega)$ will be considered as a number of the quasiparticle peaks. Our calculations for Si_7 isomers show that plasmon satellites carry about 15% of the valence spectral function weight.[46] Thus $\ln \overline{Z}$ is about 0.15 (formula (8)). For the estimation of ω_p differences, we compared the shifts of the satellites from QP peaks for Si_7 isomers. The accuracy limit of our $A(\omega)$ calculations shows that the differences between the shifts are less than 2%. This estimation is very rough. This allows us only to say that plasmonic corrections for the relative energy are less than 0.3 eV for Si_7 isomers. Because of this, the accuracy of our calculations will be examined for the test cases in Sec. IV. It will be shown that plasmonic corrections are in fact much less.

It is known that G_0W_0 QP spectrum depends on starting point wavefunction. Therefore when we calculate the total energy using the G_0W_0 method and GM formula, the results also depend on the starting point wavefunction. However, when calculating the differences of the isomers energies (in our approach we deal with energy differences only) the starting point effects are mutually compensated for the most part.

In our work, we also perform an analysis of the polarizabilities of nanoclusters. Polarizability values α were calculated using VASP and averaged over directions. Polarizabilities here are measured in relative units, where the lowest polarizability among isomers for a given formula is defined as 1. All isomer energies will be counted from the ground-state structure.

IV. ACCURACY OF CALCULATIONS AND THE INFLUENCE OF THE ENVIRONMENT

Table I presents a comparison of the total energy differences obtained by the experiment, DFT, hybrid functional, Hartree-Fock, and GM GW calculations. First part contains information on energy difference between two C_2H_6O isomers (ethyl and dimethyl ether). Second part presents data on the energy of the Si_6 nanocluster dissociation into two Si_3 nanoclusters. In Table I, PBE, HF, PBE0, and B3LYP calculations were made with the QE package; PAW and $scGW_0$—with the VASP; G_0W_0 and ev-scGW—with the BerkeleyGW.

The data in Table I show that GW energies tend to modify DFT values towards the experimental ones. GM GW energies exhibit better agreement with experiment than DFT results, upon which they are based. Accurate calculations require a large vacuum region, leading to a dramatic increase of the computational cost in the case of the plane-wave basis set. Thus the use of high parameters was restricted, especially for VASP $scGW_0$. PBE0 and B3LYP show overall rather poor energy values for the systems studied (and the worst results in the case of HF). Table I shows that PBE0 systematically demonstrates a tendency to overestimation, while B3LYP systematically shows a tendency to underestimation of the PBE results. PBE0 gives a very good result for the ethyl-dimethyl ether molecules. Errors of PBE0 and B3LYP are noticeably larger than PBE ones for the Si_6 dissociation into two Si_3 clusters. Thus hybrid functional in a few cases may improve results compared to DFT, but this seems rather occasional. Summarizing the results of Table I, we can say that the used GM GW methods give the values closest to the experiment. Comparison of G_0W_0 and ev-scGW shows that the latter method is more accurate, however G_0W_0 demonstrates noticeable improvement over PBE and hybrid functionals

TABLE I. Results for the experimental, DFT, HF, hybrid functional, and GW calculations of total energy differences for ethyl/dimethyl ether molecules and Si_6 nanocluster/two Si_3 nanoclusters.

Ethyl–dimethyl ether energy difference, eV	
Experiment	0.526
PBE/PAW	0.493/0.475
HF	0.474
PBE0	0.529
B3LYP	0.479
G_0W_0	0.504
ev-scGW/$scGW_0$	0.512/0.56
Dissociation of the nanocluster Si_6 into two Si_3, eV	
Experiment	5.82[47]
PBE	5.964
HF	4.238
PBE0	6.196
B3LYP	4.886
G_0W_0	5.697
ev-scGW	5.921

Reuse of AIP Publishing content is subject to the terms: https://publishing.aip.org/authors/rights-and-permissions. Downloaded to IP: 91.103.211.186 On: Fri, 26 Aug 2016 16:29:05

results and is relatively cheap. These facts allow G_0W_0 to be used as the main method for further calculations.

For DFT calculations of nanoclusters and molecules, the size of vacuum region needed to converge is usually referred to 7-10 Å (for systems with zero net charge).[62,63] Because of the dynamical nature of the xc interaction, GW should be sensitive to the induced dipole-dipole interactions or dispersion interaction. This interaction could be significant at distances of about 10 Å. Besides, in practical applications, nanoclusters could be embedded in a matrix and form a periodic structure, where the period value would affect system properties. It is of interest to study the dependence of the system energetics convergence on the vacuum region and the supercell size.

Table II presents energy ordering for the first four Si_7 isomers inside 8.5, 10.5, 13.2, 18.5, 23.8 Å cubic supercells. The number at the top of each column in Table II denotes the actual structure. For the 8.5 Å supercell, relative polarizabilities are also presented.

Change in supercell size noticeably affects isomer energy ordering in G_0W_0 and $scGW_0$ methods. In 8.5 Å supercell, the structure 2 has much lower energy than other isomers. For 10.5 Å supercell and larger, the structure 1 becomes the ground-state isomer. Polarizability analysis shows that structure 2 in the 8.5 Å supercell has much less α than other structures. For the supercells larger than 8.5 Å, isomers' polarizabilities have small differences and do not make a noticeable contribution to the energy ordering of clusters. Such energy rearrangement of the structures in 8.5 Å supercell is associated with the increase of the interaction of clusters in neighboring supercells. Other numerical methods in Table II do not show such rearrangements since structure 1 is the ground-state isomer for all supercells. Basically PBE0 and B3LYP show tendencies to overestimation and underestimation of the PBE results, respectively, as it was mentioned above.

Table II shows that for the GW approach, the increase in the supercell size leads not only to a monotonic convergence of the relative energies of the isomers. It could be seen, that structures number 2 and 3 alternately change places on the energy scale when the supercell changes from 8.5 to 10.5 Å, from 10.5 to 13.2 Å, from 13.2 to 18.5 Å. Only for the supercell 18.5 Å this alternation stops and for 23.8 Å supercell it is possible to say that convergence is achieved. Such behavior indicates a complex nature of the decrease in screened Coulomb interaction with distance in nanoclusters.

For supercell sizes above 13.2 Å (about 9 Å of vacuum), PBE relative energies are converged to within 0.2% and

TABLE II. PBE, PBE0, B3LYP, BerkeleyGW G_0W_0, VASP $scGW_0$ energies, and polarizabilities in relative units for the first four Si_7 isomers in the 8.5 Å–23.8 Å cubic supercells.

Isomer number	1	2	3	4
8.5 Å cubic supercell				
PBE, eV	0	0.17	0.412	0.416
PBE0, eV	0	0.214	0.436	0.441
B3LYP, eV	0	0.011	0.246	0.256
G_0W_0, eV	0.944	0	0.82	0.833
$scGW_0$, eV	1.207	0	0.995	1.024
α	1.472	1	1.452	1.215
10.5 Å cubic supercell				
PBE, eV	0	0.7481	0.9878	0.7865
PBE0, eV	0	0.7491	1.0426	0.7815
B3LYP, eV	0	0.5699	0.7484	0.6072
G_0W_0, eV	0	0.4669	0.4473	0.5452
13.2 Å cubic supercell				
PBE, eV	0	0.8067	0.9898	0.8079
PBE0, eV	0	0.8006	1.0458	0.8057
B3LYP, eV	0	0.6252	0.7504	0.6311
G_0W_0, eV	0	0.6419	0.6854	0.75
18.5 Å cubic supercell				
PBE, eV	0	0.8091	0.9904	0.8093
PBE0, eV	0	0.8134	1.0484	0.8148
B3LYP, eV	0	0.636	0.7525	0.6387
G_0W_0, eV	0	0.7406	0.7109	0.7769
23.8 Å cubic supercell				
PBE, eV	0	0.8092	0.9904	0.8094
PBE0, eV	0	0.8159	1.0487	0.8162
B3LYP, eV	0	0.6381	0.7529	0.6399
G_0W_0, eV	0	0.745	0.7017	0.7747

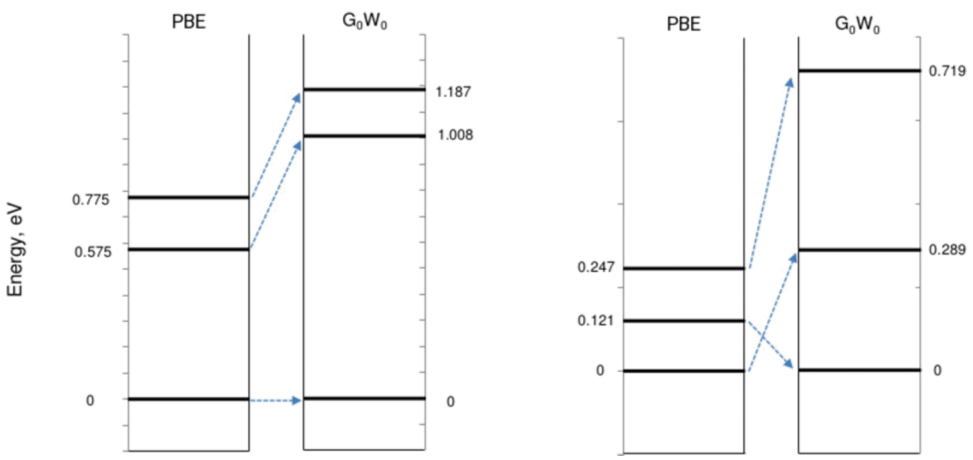

FIG. 2. Si_{10} (left) and $Si_{10}H_6$ (right) isomers relative energies in PBE and G_0W_0.

Reuse of AIP Publishing content is subject to the terms: https://publishing.aip.org/authors/rights-and-permissions. Downloaded to IP: 91.103.211.186 On: Fri, 26 Aug 2016 16:29:05

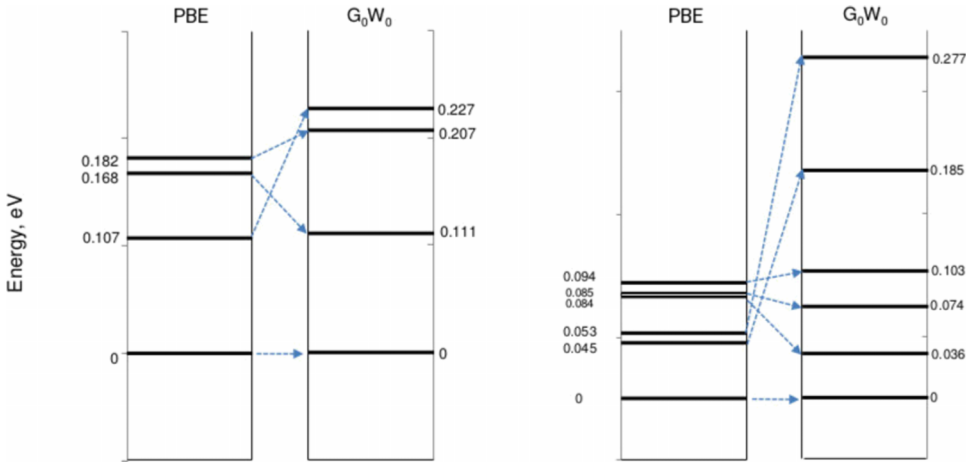

FIG. 3. $Si_{10}H_{16}$ (left) and $Si_{10}H_{22}$ (right) isomers relative energies in PBE and G_0W_0.

within 1% for the PBE0 and B3LYP. GW relative energies show slower convergence, the convergence of energy at a level of accuracy within one percent requires an increase in vacuum region up to 15 Å.

V. ELECTRON CORRELATION EFFECTS IN $Si_{10}H_{2n}$ AND ISOMER ENERGY DISTRIBUTION

Figures 2-5 demonstrate the relative positions of energy levels for Si_{10}, $Si_{10}H_6$, $Si_{10}H_{12}$, $Si_{10}H_{16}$, $Si_{10}H_{20}$, $Si_{10}H_{22}$ nanocluster isomers. The size of the vacuum region was set to 13 Å. Figs. 2 and 3 present DFT PBE calculations (left parts) and G_0W_0 PBE calculations (right parts) for Si_{10}, $Si_{10}H_6$, $Si_{10}H_{16}$, $Si_{10}H_{22}$ nanoclusters. Figs. 4 and 5 present PBE, PBE0, B3LYP, Hartree-Fock, and G_0W_0 PBE calculations for $Si_{10}H_{12}$ and $Si_{10}H_{20}$ isomers. It can be seen that in most cases, G_0W_0 isomer energies change their relative ordering comparing to the PBE results. PBE0 energies are consistent with PBE ones. B3LYP and Hartree-Fock calculations exhibit some differences from PBE but also give no results consistent with GW (even on a qualitative level). We also made PBE0 calculations with different mixing constant α_{mix} for the xc term (see formula (3)). Computations with α_{mix} varied from 0 to 1 just reproduce the results close to PBE or HF and give no conceptually new results. For $Si_{10}H_6$ and $Si_{10}H_{12}$ isomers (Figs. 2 and 4), G_0W_0 ground-state structures also differ from PBE and hybrid functionals. In most cases, the energy spread of the isomers in GWA is larger than in DFT.

Figure 6 presents values of the polarizability α and total energy from PBE and Galitskii-Migdal G_0W_0 calculations. Each part in Fig. 6 shows results for isomers of a given formula: Si_{10}, $Si_{10}H_6$, $Si_{10}H_{12}$, $Si_{10}H_{16}$, $Si_{10}H_{20}$, and $Si_{10}H_{22}$. As can be seen, Si_{10}, $Si_{10}H_6$, $Si_{10}H_{12}$, and $Si_{10}H_{16}$ clusters in GM GWA mainly have lower total energy (more stable) for the isomers with lower α. The PBE calculations do not exhibit such apparent energy-polarizability correlation. One can note violation of this rule for $Si_{10}H_6$ isomers: for the GW energy-polarizability curve structure with $\alpha = 1$ (point marked as 1) has energy of 0.3 eV higher than the structure with $\alpha = 1.012$ (mark 2). Calculations of $Si_{10}H_{2n}$ clusters' dipole moments show that the structure marked as 1 has dipole moment of 1.2 atomic units, the largest value of all clusters examined. Other clusters have 4-100 times lower dipole moments. Apparently such a large dipole moment affects the energy of structure 1, decreasing its stability.

The situation for the energy-polarizability correlation changes with increasing hydrogenation. For $Si_{10}H_{20}$ and $Si_{10}H_{22}$ clusters, there is no correlation between α and GM total energy value. This behavior can be explained as follows: for the $Si_{10}H_{2n}$ clusters with $n < 9$, an inner Si core can be localized; increasing n, we get clusters of loose structure with no inner part (see Figure 1). In case of $Si_{10}H_{20}$ and $Si_{10}H_{22}$ isomers, the structure is branched, rather one-dimensional for each branch. In Refs. 64–66, it was pointed out that in

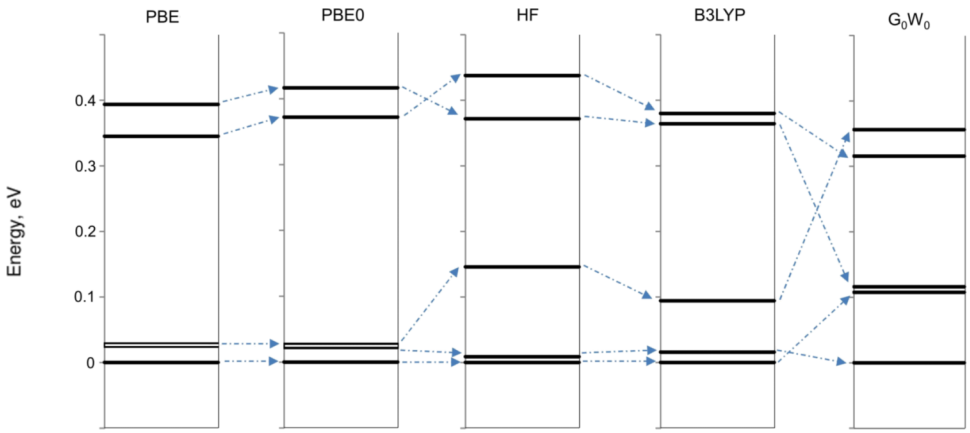

FIG. 4. $Si_{10}H_{12}$ isomers relative energies in PBE, PBE0, HF, B3LYP, and G_0W_0.

Reuse of AIP Publishing content is subject to the terms: https://publishing.aip.org/authors/rights-and-permissions. Downloaded to IP: 91.103.211.186 On: Fri, 26 Aug 2016 16:29:05

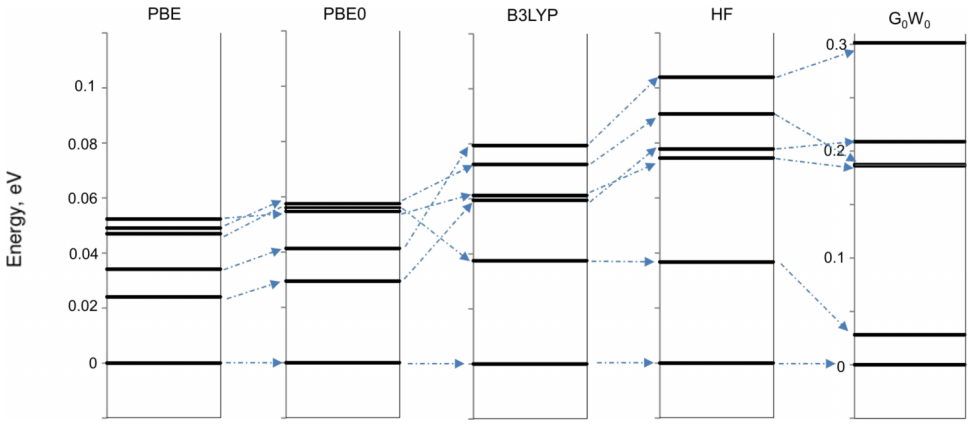

FIG. 5. $Si_{10}H_{20}$ isomers relative energies in PBE, PBE0, HF, B3LYP, and G_0W_0. The right graph for the G_0W_0 results has different scale.

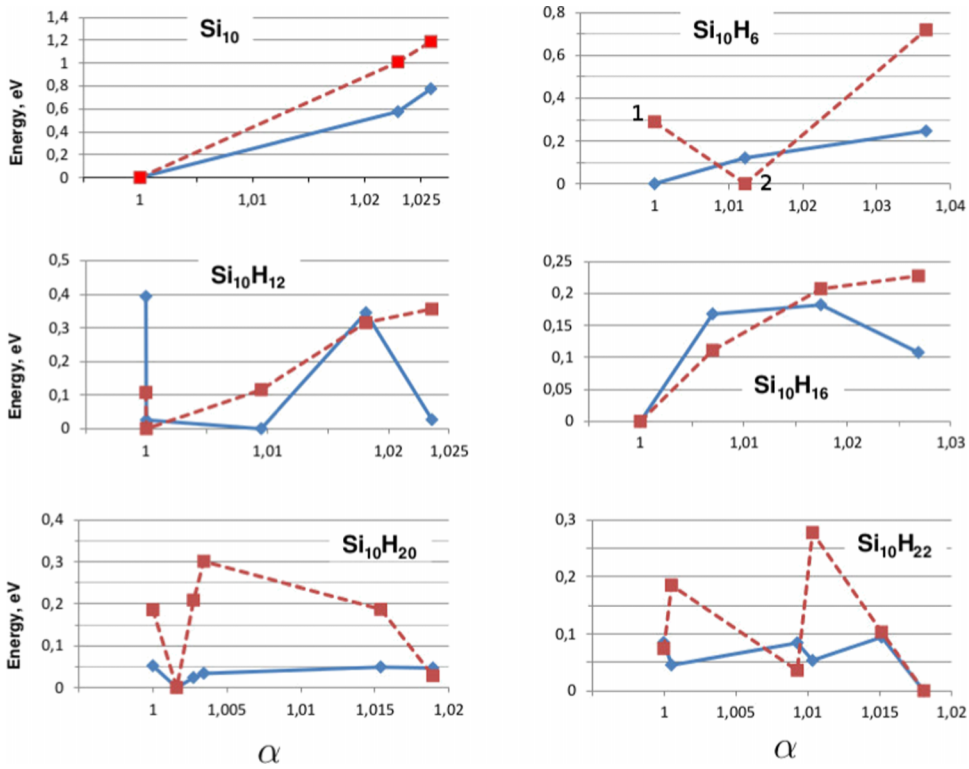

FIG. 6. Si_{10}, $Si_{10}H_6$, $Si_{10}H_{12}$, $Si_{10}H_{16}$, $Si_{10}H_{20}$, $Si_{10}H_{22}$ isomers' polarizability and total energy from PBE (diamonds, solid line) and G_0W_0 (boxes, dashed line).

small clusters, microscopic dielectric properties a few atomic distances away from the surface are almost identical to the bulk ones, whereas the surface is one of the main factors that significantly change cluster polarizability. Thus $Si_{10}H_{2n}$ clusters with clearly defined inner part show standard relation between system polarizability and energetics, while branched structures do not exhibit such obvious relations.

VI. CONCLUSIONS

DFT, hybrid functionals, Hartree-Fock, Galitskii-Migdal GW approximations (without account for satellite) were applied to total energy computations of silicon-hydrogen nanoclusters. The accuracy of the methods was tested for the cases of the energy difference for ethyl-dimethyl ether isomers and the energy of the Si_6 nanocluster dissociation into two Si_3 nanoclusters. GM GW gives the most accurate results of all methods examined. GW energy calculations also demonstrate significantly higher sensitivity to the nanocluster environment, with convergence of cluster energies requiring much thicker vacuum region than DFT. Moreover a non-monotonic dependence of the isomers energy distribution on supercell size was found.

Total energy calculations of Si_7 and $Si_{10}H_{2n}$ isomers show that correct account for electron correlation effects is of great importance when energy differences between isomer structures are small. Comparing to other methods applied, GWA demonstrates a notable change in the isomers' energy ordering and gives a correction to the energy of the order of tenths of eV. Such correction will be significant for the energy ranking of the competitive structures up to a temperature of ~1000 K. It seems reasonable to expect that the correct description of the electron correlations will be equally important in the energetics of any nanoclusters consisting of tens of atoms, where the number of surface

Reuse of AIP Publishing content is subject to the terms: https://publishing.aip.org/authors/rights-and-permissions. Downloaded to IP: 91.103.211.186 On: Fri, 26 Aug 2016 16:29:05

atoms is comparable to the number of inner atoms that leads to noticeable contribution to the energy of the system from the surface.

It was found that for compact clusters the most stable structure tends to have the lowest mean polarizability. In the branched, loosely packed structures such correlation disappears. We expect that the minimal polarizability principle can be a valid criterion for isomer stability when considering large nanoclusters, unaffordable for GW calculations.

ACKNOWLEDGMENTS

This work was supported by Programmes of the Russian Academy of Sciences and Russian Foundation for Basic Research (Grant Nos. 16-32-00922, 16-02-00024, and 16-02-00612), the Project 5-100 grant of the Russian Government to MIPT. We would like to thank Yu. A. Uspenskii for useful discussions.

[1]V. Kumar, *Nanosilicon*, 1st ed. (Elsevier, Amsterdam, 2007).
[2]*Silicon Nanophotonics*, edited by L. Khriachtchev (World Scientific Publishing, Singapore, 2009).
[3]N. O'Farrel, A. Houlton, and B. Horrocks, Int. J. Nanomed. **4**, 451–472 (2006).
[4]W. L. Wilson, P. F. Szajowski, and L. E. Brus, Science **262**, 1242 (1993).
[5]G. Belomoin *et al.*, Appl. Phys. Lett. **80**, 841 (2002).
[6]J. Oviedo and R. E. Palmer, J. Chem. Phys. **117**, 9548 (2002).
[7]A. Puzder, A. J. Williamson, F. Gygi, and G. Galli, Phys. Rev. Lett. **92**, 217401 (2004).
[8]C. Li, W. Guo, Y. Kong, and H. Gao, Appl. Phys. Lett. **90**, 223102 (2007).
[9]W. Kohn and L. J. Sham, Phys. Rev. **140**, A1133 (1965).
[10]J. P. Perdew, K. Burke, and Y. Wang, Phys. Rev. B **54**, 16533 (1996).
[11]V. S. Baturin, S. V. Lepeshkin, N. L. Matsko, A. R. Oganov, and Yu. A. Uspenskii, EPL **106**, 37002 (2014).
[12]V. S. Baturin *et al.*, J. Phys.: Conf. Ser. **510**, 012032 (2014).
[13]J. C. Grossman and L. Mitas, Phys. Rev. Lett. **74**, 1323 (1995).
[14]J. C. Grossman and L. Mitas, Phys. Rev. B **52**, 16735 (1995).
[15]L. Mitas, J. C. Grossman, I. Stich, and J. Tobik, Phys. Rev. Lett. **84**, 1479 (2000).
[16]M. Luppi and S. Ossicini, Phys. Rev. B **71**, 035340 (2005).
[17]H. Wang, J. Sun, W. C. Lu *et al.*, J. Phys. Chem. C **112**, 7097-7101 (2008).
[18]M. C. Caputo, O. Ona, and M. B. Ferraro, J. Chem. Phys. **130**, 134115 (2009).
[19]S. X. Hu, J. G. Yu, and E. Y. Zeng, J. Phys. Chem. A **114**, 10769-10774 (2010).
[20]H. B. Du, S. P. Huang, A. De Sarkar *et al.*, J. Chem. Phys. A **118**(39), 8893-8900 (2014).
[21]A. D. Becke, J. Chem. Phys. **98**(2), 1372–1377 (1993).
[22]J. P. Perdew, M. Ernzerhof, and K. Burke, J. Chem. Phys. **105**, 9982 (1996).
[23]C. Adamo and V. Barone, J. Chem. Phys. **110**(13), 6158–6170 (1999).
[24]A. D. Becke, J. Chem. Phys. **98**(7), 5648–5652 (1993).
[25]K. Kim and K. D. Jordan, J. Phys. Chem. **98**(40), 10089–10094 (1994).
[26]P. J. Stephens, F. J. Devlin, C. F. Chabalowski, and M. J. Frisch, J. Phys. Chem. **98**(45), 11623–11627 (1994).
[27]J. Heyd, G. E. Scuseria, and M. Ernzerhof, J. Chem. Phys. **118**(18), 8207 (2003).
[28]A. B. Migdal, Sov. Phys. JETP **5**, 333 (1957), http://www.jetp.ac.ru/cgi-bin/index2/gf-view/en/a-b-migdal-the-momentum-distribution-of-interacting-fermi-particles-sov-phys-jetp-333-1957.
[29]V. M. Galitskii and A. B. Migdal, Sov. Phys. JETP **7**, 96 (1958), http://www.jetp.ac.ru/cgi-bin/e/index/e/7/1/p96?a=list.
[30]B. Holm and F. Aryasetiawan, Phys. Rev. B **62**, 4858 (2000).
[31]L. Hedin and S. Lundqvist, Solid State Phys. **23**, 1 (1970).
[32]F. Caruso, H. Lambert, and F. Giustino, Phys. Rev. Lett. **114**, 146404 (2015).
[33]D. C. Langreth and J. P. Perdew, Solid State Commun. **17**, 1425 (1975).
[34]O. Gunnarsson and B. I. Lundqvist, Phys. Rev. B **13**, 4274 (1976).
[35]Y. M. Niquet, M. Fuchs, and X. Gonze, Phys. Rev. A **68**, 032507 (2003).
[36]P. Giannozzi *et al.*, J. Phys.: Condens. Matter **21**, 395502 (2009).
[37]G. Kresse and J. Hafner, Phys. Rev. B **47**, 558 (1993).
[38]G. Kresse and J. Hafner, Phys. Rev. B **49**, 14251 (1994).
[39]G. Kresse and J. Furthmuller, Comput. Mater. Sci. **6**, 15 (1996).
[40]G. Kresse and J. Furthmuller, Phys. Rev. B **54**, 11169 (1996).
[41]P. E. Blochl, Phys. Rev. B **50**, 17953 (1994).
[42]G. Kresse and D. Joubert, Phys. Rev. B **59**, 1758 (1999).
[43]A. R. Oganov and C. W. Glass, J. Chem. Phys. **124**, 244704 (2006).
[44]A. R. Oganov, A. O. Lyakhov, and M. Valle, Acc. Chem. Res. **44**, 227-237 (2011).
[45]M. S. Hybertsen and S. G. Louie, Phys. Rev. B **34**, 5390 (1986).
[46]Note: About 10% in case of dimethyl ether molecule.
[47]Note: The value obtained from the binding energies for Si_6 and Si_3 from Ref. 13.
[48]F. Caruso, D. R. Rohr, M. Hellgren, X. Ren, P. Rinke, A. Rubio, and M. Scheffler, Phys. Rev. Lett. **110**, 146403 (2013).
[49]E. V. Tikhonov, Yu. A. Uspenskii, and D. R. Khokhlov, JETP **120**(6), 1093 (2015).
[50]R. Guerra, I. Marri, R. Magri, L. Martin-Samos, O. Pulci, E. Degoli, and S. Ossicini, Phys. Rev. B **79**, 155320 (2009).
[51]G. Baym and L. P. Kadanoff, Phys. Rev. **124**, 287 (1961).
[52]G. Baym, Phys. Rev. **127**, 1391 (1962).
[53]B. Holm, Phys. Rev. Lett. **83**, 788 (1999).
[54]A. Stan, N. E. Dahlen, and R. van Leeuwen, EPL **76**(2), 298-304 (2006).
[55]F. Caruso, P. Rinke, X. Ren, M. Scheffler, and A. Rubio, Phys. Rev. B **86**, 081102(R) (2012).
[56]B. Holm and U. von Barth, Phys. Rev. B **57**, 2108 (1998).
[57]W.-D. Schone and A. G. Eguiluz, Phys. Rev. Lett. **81**, 1662 (1998).
[58]K. Delaney, P. Garcia-Gonzalez, A. Rubio, P. Rinke, and R. W. Godby, Phys. Rev. Lett. **93**, 249701 (2004).
[59]G. Onida, L. Reining, and A. Rubio, Rev. Mod. Phys. **74**, 601 (2002).
[60]M. Rohlfing and S. G. Louie, Phys. Rev. B **62**, 4927 (2000).
[61]J. Deslippe, G. Samsonidze, D. A. Strubbe, M. Jain, M. L. Cohen, and S. G. Louie, Comput. Phys. Commun. **183**, 1269 (2012); e-print arXiv:1111.4429.
[62]W. Luo, S. J. Pennycook, and S. T. Pantelides, Nano Lett. **7**(10), 3134–3137 (2007).
[63]G. M. Faccin and E. Z. da Silva, J. Cluster Sci. **23**(4), 953-966 (2012).
[64]C. Delerue, M. Lannoo, and G. Allan, Phys. Rev. B **68**, 115411 (2003).
[65]H. Y. Kim, J. O. Sofo, D. Velegol, M. W. Cole, and G. Mukhopadhyay, Phys. Rev. A **72**, 053201 (2005).
[66]A. Franceschetti and M. C. Troparevsky, Phys. Rev. B **72**, 165311 (2005).

Reuse of AIP Publishing content is subject to the terms: https://publishing.aip.org/authors/rights-and-permissions. Downloaded to IP: 91.103.211.186 On: Fri, 26 Aug 2016 16:29:05